Chapter 4

Heavy charged Higgs Boson decaying into top quark in the MSSM

The SUSY (QCD and leading electroweak) one-loop corrections to the charged Higgs decay into top quark are discussed in a framework in which $\tan\beta$ is large and defined through $\Gamma(H^+ \to \tau^+\nu_\tau)$. We show that a measurement of the BR$(H^+ \to \tau^+\nu_\tau)$, either at the TEVATRON or at the LHC, with a modest precision of $\sim 20\%$ could be sufficient to unravel the SUSY underlying nature of a charged Higgs.

4.1 Motivation

Observing a heavy charged Higgs boson produced in the near future at the Tevatron or at the LHC would be instant evidence of physics beyond the Standard Model. Whether such Higgs bosons are supersymmetric or not can not be disentangled with only a simple tree-level study of $H^+ \to t\bar{b}$. Such a study would be blind to the nature of the Higgs sector to which H^+ belonged. It is clear that a careful study of the quantum effects on $H^+ \to t\bar{b}$ could be the clue to unravel the potential supersymmetric nature of the charged Higgs; in particular, it should be useful to distinguish it from a charged Higgs belonging to a general two-Higgs

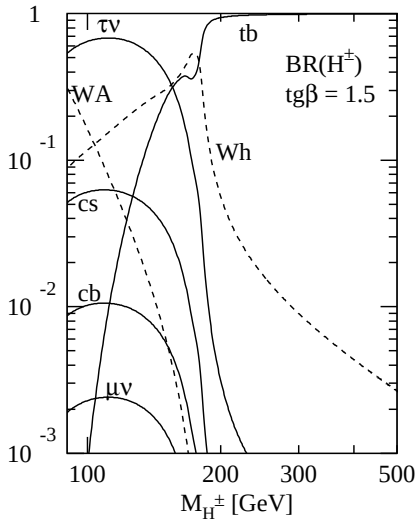

Figure 4.1: *Charged Higgs decay branching ratios at tree level [113].*

doublet model.

The charged Higgs boson can decay hadronically into several quark final states, and if it is sufficiently heavy it can also decay into top and bottom quarks. It is natural, and necessary due to the QCD radiative effects nature, to tackle their effects on $H^+ \to t\bar{b}$ first. These conventional QCD corrections were first considered in Ref. [114, 115] and they are known to be large and negative in the limit of Higgs masses much bigger than the quark masses –which is the region we will be interested in-. In spite of the huge size of the standard QCD corrections for light quark final states, it is clear that these channels are severely suppressed by the small Yukawa couplings $g\, m_q/M_W \ll 1 (\text{for } q = u, d, c, s)$ and/or by off-diagonal CKM matrix elements, so that their branching fractions are very tiny (Fig. 4.1). Therefore, as soon as the $t\,\bar{b}$ threshold is open ($M_{H^+} > m_t + m_b \sim 180\, GeV$) one is left with $H^+ \to t\bar{b}$ as the only relevant hadronic decay of a heavy charged Higgs boson. The conventional QCD corrections to that decay [114–117] cannot distinguish the nature of the underlying Higgs model, but their knowledge is indispensable to probe the existence of additional sources of strong quantum effects beyond the SM.

In this chapter we will show the effects of the leading electroweak corrections originating from large Yukawa couplings within the MSSM as well as the $\widetilde{\text{QCD}}$ quantum effects mediated

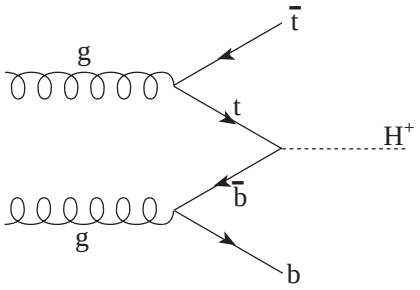

(a)

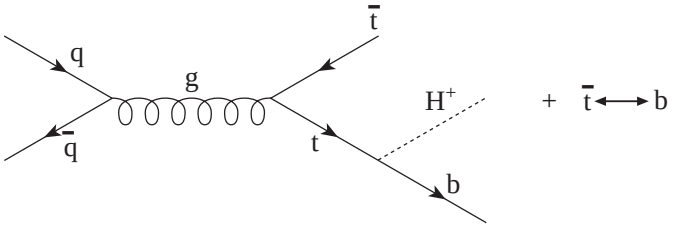

(b)

Figure 4.2: *Typical charged-Higgs production mechanisms at hadron colliders:* **(a)** H^+ *production through* $t\bar{b}$*-fusion; and* **(b)** *through charged Higgs bremsstrahlung off top and bottom quarks.*

by squarks and gluinos and shall compare them two with the standard QCD corrections to the decay $H^+ \to t\bar{b}$. We will show that not only the $\widetilde{\text{QCD}}$ corrections but also the $\widetilde{\text{EW}}$ turn out to be of comparable size to the $\mathcal{O}(\alpha_s)$ QCD in "relevant" portions of the MSSM parameter space rendering it possible for a hadron collider to show vestiges of virtual SUSY signatures.

Nevertheless, not only is the decay $H^+ \to t\bar{b}$ important in itself to try to unravel the nature of the symmetry breaking mechanism and/or elucidating the Quantum Field Theory under the SM, if any, but the $H^\pm\, t\,b$-vertex responsible for it could be also at the root of the Higgs production mechanism itself. For, one expects that e.g. H^+ (similarly for H^-) can be

generously produced in hadron machines through $t\,\bar{b}$-fusion, $g\,g \to H^+\,\bar{t}\,b$ (Fig. 4.2a), as well as from charged Higgs bremsstrahlung off top and bottom quarks, $q\,\bar{q} \to H^+\,\bar{t}\,b$ (Fig. 4.2b), as we have recently shown [44, 45] –Notice that trigging on a top quark in association is very useful to avoid the signal being swamped by the huge backgrounds. While the first mechanism is to be dominant at the LHC, and would allow to produce annually around $10^4 - 10^6$ charged Higgs particles of a mass comprised between a few hundred GeV up to about 1 TeV for a luminosity of $\mathcal{L} \sim 10^{34}\,cm^{-2}\,s^{-1}$ [118]; the second one could still give a chance to Tevatron, where Drell-Yan production of $t\,\bar{t}$ and $b\,\bar{b}$ are the primary processes. Moreover, contrary to what might seem, the latter processes (Fig. 4.2b) are not necessarily too suppressed against the ordinary two-body mode $q\,q' \to W^* \to t\,\bar{b}$ as this amplitude is purely electroweak, i.e. of $\mathcal{O}(\alpha_W)$, whereas the former involves a three-body final state, but in compensation it is of order $\mathcal{O}(\alpha_s\,\lambda_b\sqrt{\alpha}_W)$; and so at large $\tan\beta$ (where $\lambda_b > 1$) it does afford a contribution of comparable size [44, 45].

We point out, in passing, that the diagrams in Fig. 4.2b also contribute to the cross-section for single top-quark production, whose measurement is one of the main goals at the next Tevatron run (Run II). The complete list of gg fusion diagrams can be seen in Fig. 4.3. It is clear that these production mechanisms could be rather efficient in the colliders, for the $H^+\,t\,\bar{b}$-vertex can be strongly enhanced and result in a very distinctive phenomenology as compared to the experimental expectations for the SM Higgs production, typically through (one-loop) $g\,g$-fusion [119–121]. Most important, as we will see in detail, in the MSSM the $H^+\,t\,\bar{b}$-vertex can receive significant corrections (in some cases of order 50%) which could play a decisive role to disentangle whether a charged Higgs hypothetically produced in a hadron collider is supersymmetric or not.

In both production mechanisms one relies on the possibility of enhanced Yukawa couplings of the charged Higgs boson with top and bottom quarks (eq. 2.5):

$$\lambda_t \equiv \frac{h_t}{g} = \frac{m_t}{\sqrt{2}\,M_W\,\sin\beta} \quad , \quad \lambda_b \equiv \frac{h_b}{g} = \frac{m_b}{\sqrt{2}\,M_W\,\cos\beta}\,.$$

And it is this requirement that automatically gives large $\widetilde{\mathrm{EW}}$ corrections as will be seen.

However, the very same SUSY parameters that govern the behaviour of the quantum effects that we will be studying are relevant to the low-energy physics of the radiative $\bar{B}^0$-

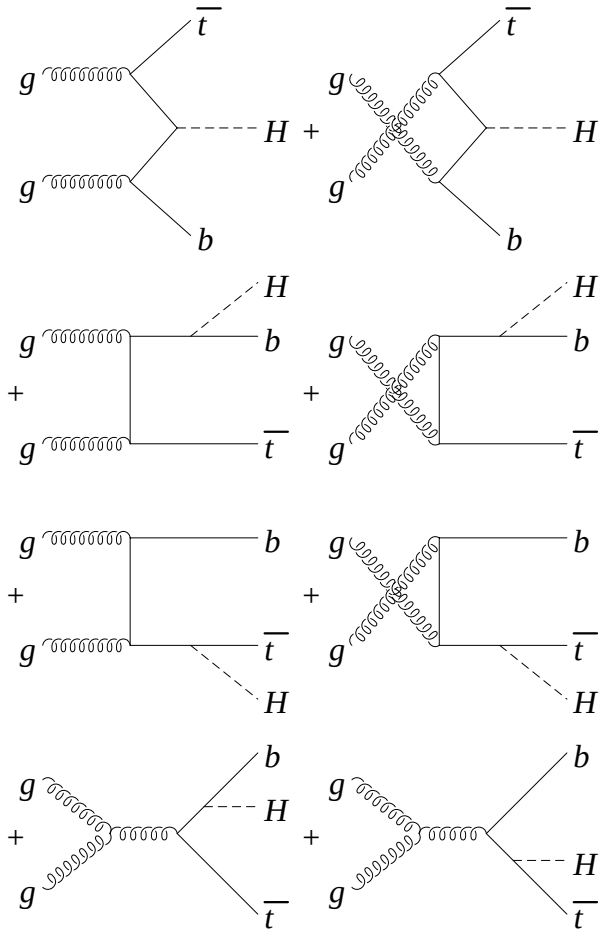

Figure 4.3: *Single top quark production through gluon fusion ($gg \to H^+\bar{t}b$) mechanisms in associatiation with charged Higgs at hadron colliders [44].*

decays $b \to s\gamma$. Therefore, the severe constraints imposed by this process cannot be ignored for the study of the charged Higgs decay and we will make use of them to pinpoint the aforementioned "relevant" portions of the MSSM parameter. To this end, as will be explained in more detail, we have used –and checked– the LO formula (see the extensive literature [122–129] for details):

$$BR(b \to s\,\gamma) \simeq BR(b \to c\,e\,\bar{\nu})\,\frac{(6\,\alpha_{\rm em}/\pi)\,\left(\eta^{16/23}\,A_\gamma + C\right)^2}{I(m_c/m_b)\,\left[1 - \frac{2}{3\pi}\,\alpha_s(m_b) f_{\rm QCD}(m_c/m_b)\right]}\,,$$

where

$$A_\gamma = A_{\rm SM} + A_{H^-} + A_{\chi^-\tilde{q}}$$

is the sum of the SM, charged Higgs and chargino-squark amplitudes, respectively. Although the NLO QCD corrections to the SM (W-mediated) and charged Higgs mediated amplitudes are already available (see e.g. Refs. [130, 131]), our results would not significantly change by using these more complete calculations.

4.2 Lowest order relations and experimental situation

As explained above and seen in Fig. 4.1, the charged Higgs decay $H^+ \to t\bar{b}$ is expected to be the dominant when the $t\,\bar{b}$ threshold is open ($M_{H^+} > m_t + m_b \sim 180\,GeV$). This derives from the following formulae and is further analyzed below.

The interaction lagrangian describing the $H^+\,t\,\bar{b}$-vertex in the MSSM reads:

$$\mathcal{L}_{Htb} = \frac{g\,V_{tb}}{\sqrt{2}M_W}\,H^+\,\bar{t}\,[m_t\cot\beta\,P_L + m_b\tan\beta\,P_R]\,b + \text{h.c.}\,, \tag{4.1}$$

where $P_{L,R} = 1/2(1 \mp \gamma_5)$ are the chiral projector operators and V_{tb} is the corresponding CKM matrix element –henceforth we set $V_{tb} = 1$ since from unitarity of the CKM-matrix, under the assumption of three generations, $V_{tb} = 0.999$ within $\pm 0.1\%$.

This implies for the partial charged Higgs decay width into $t\bar{b}$ at tree level in the α parametrization:

$$\Gamma_\alpha^{(0)} = \left(\frac{\alpha}{s_W^2}\right)\,\frac{D}{16\,M_W^2\,m_t}\,\lambda^{1/2}(1, \frac{m_b^2}{m_t^2}, \frac{M_{H^\pm}^2}{m_t^2})\,, \tag{4.2}$$

where

$$D = (M_{H^\pm}^2 - m_t^2 - m_b^2)\,(m_t^2 \cot^2\beta + m_b^2 \tan^2\beta) - 4 m_t^2 m_b^2\,,$$

and In the G_F-parametrization it reads:

$$\Gamma^{(0)}_{G_F} = \left(\frac{G_F}{8\pi\sqrt{2}}\right) \frac{D}{m_t}\, \lambda^{1/2}(1, \frac{m_b^2}{m_t^2}, \frac{M_{H^\pm}^2}{m_t^2})\,, \tag{4.3}$$

The fact that, when the $t\,\bar{b}$ threshold is open ($M_{H^+} > m_t + m_b \sim 180\,GeV$), the charged Higgs decay $H^+ \to t\bar{b}$ is expected to be the dominant is further shown in Fig 4.4, where it has been also made evident that the $\tau\nu_\tau$ charged Higgs decay is non negligible even for $M_{H^\pm} \approx 500\,\mathrm{GeV}$. This fact turns out to be of paramount importance given the chosen $\tan\beta$ renormalization framework.

4.2.1 Experimental constraints. The $b \to s\gamma$ constraint

As mentioned above the $b \to s\gamma$ decay plays a fundamental role in constraining the MSSM parameter space. In this section we will illustrate the effect of the variation of the different MSSM input parameters on the $b \to s\gamma$ branching ratio and then we will use this constraint together with the other generic constraints for the MSSM parameters stated in section 2.2.1 to give the relevant MSSM parameter regions in which to carry out our calculation.

The $b \to s\gamma$ decay in the MSSM

To this end reason, we have used and checked the LO formula:

$$BR(b \to s\,\gamma) \simeq BR(b \to c\,e\,\bar{\nu})\, \frac{(6\,\alpha_{\mathrm{em}}/\pi)\,\left(\eta^{16/23}\,A_\gamma + C\right)^2}{I(m_c/m_b)\,\left[1 - \frac{2}{3\pi}\,\alpha_s(m_b) f_{\mathrm{QCD}}(m_c/m_b)\right]}\,, \tag{4.4}$$

which has been under exhaustive studies in [122–129]. There

$$A_\gamma = A_{\mathrm{SM}} + A_{H^-} + A_{\chi^-\tilde{q}} \tag{4.5}$$

is the sum of the SM, charged Higgs and chargino-squark amplitudes, respectively. Explicitly:

$$SM: \qquad A_\gamma = \frac{3}{2}\frac{m_t^2}{m_W^2} f_\gamma^{(1)}\left(\frac{m_t^2}{m_W^2}\right)$$

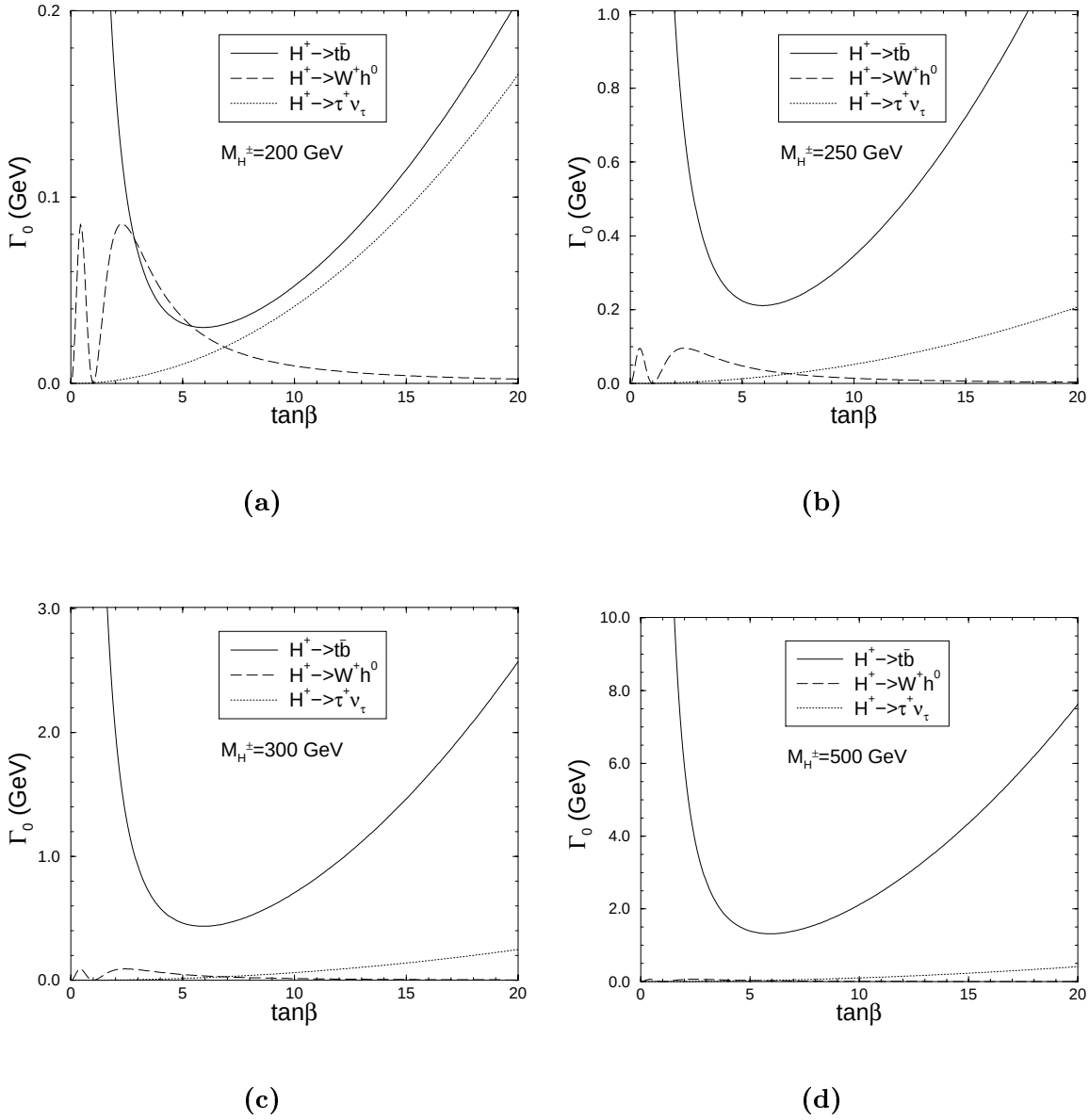

Figure 4.4: *Heavy Charged Higgs partial decay widths [47] as a function of* $\tan\beta$ *for several Higgs masses.*

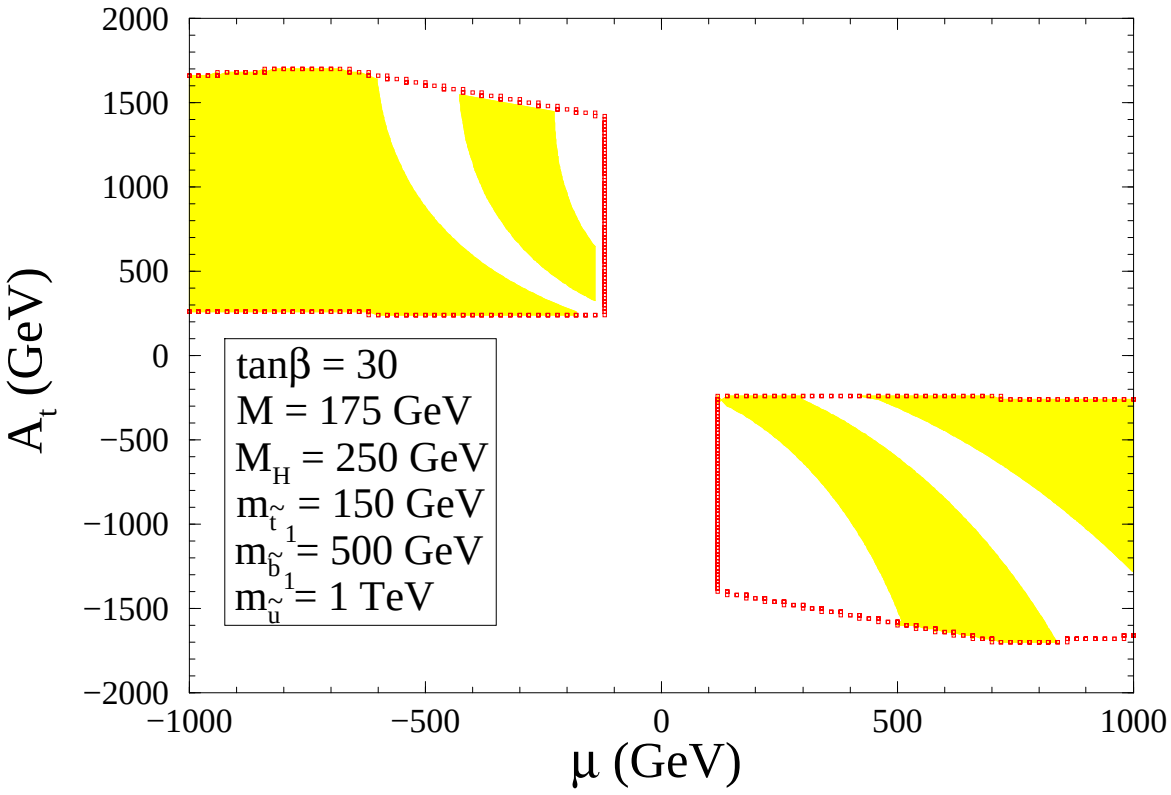

Figure 4.5: *Domains of the MSSM parameter space in the* (μ, A_t)*-plane allowed by* $b \to s\,\gamma$ *at* $2\,\sigma$ *level and the theoretical constraints explained in the text, for given values of the other parameters. The proper domains are the shaded ones.*

$$
\begin{aligned}
H^{\pm}: \qquad A_\gamma &= \frac{1}{2}\frac{m_t^2}{m_H^2}\left[\frac{1}{\tan^2\beta} f_\gamma^{(1)}\left(\frac{m_t^2}{m_H^2}\right) + f_\gamma^{(2)}\left(\frac{m_t^2}{m_H^2}\right)\right] \\
\tilde{\chi}-\tilde{q}: \qquad A_\gamma &= \sum_{j=1}^{2}\left\{\frac{m_W^2}{\tilde{m}_{\chi_j}^2}\left[|U_{j1}|^2 f_\gamma^{(1)}\left(\frac{\tilde{m}^2}{\tilde{m}_{\chi_j}^2}\right)\right.\right. \\
&\quad - \sum_{k=1}^{2}\left|U_{j1}R_{1k} - U_{j2}R_{2k}\frac{m_t}{\sqrt{2}m_W\sin\beta}\right|^2 f_\gamma^{(1)}\left(\frac{\tilde{m}_{t_k}^2}{\tilde{m}_{\chi_j}^2}\right)\Bigg] \\
&\quad - \frac{V_{j2}}{\sqrt{2}\cos\beta}\frac{m_W}{\tilde{m}_{\chi_j}}\left[U_{j1} f_\gamma^{(3)}\left(\frac{\tilde{m}^2}{\tilde{m}_{\chi_j}^2}\right)\right. \\
&\quad \left.\left. - \sum_{k=1}^{2}\left(U_{j1}R_{1k} - U_{j2}R_{2k}\frac{m_t}{\sqrt{2}m_W\sin\beta}\right) R_{1k}^* f_\gamma^{(3)}\left(\frac{\tilde{m}_{t_k}^2}{\tilde{m}_{\chi_j}^2}\right)\right]\right\}, \qquad (4.6)
\end{aligned}
$$

where:

$$
\begin{aligned}
f_\gamma^{(1)}(x) &= \frac{(7-5x-8x^2)}{36(x-1)^3} + \frac{x(3x-2)}{6(x-1)^4}\log x \\
f_\gamma^{(2)}(x) &= \frac{(3-5x)}{6(x-1)^2} + \frac{(3x-2)}{3(x-1)^3}\log x \qquad (4.7) \\
f_\gamma^{(3)}(x) &= (1-x) f_\gamma^{(1)}(x) - \frac{x}{2} f_\gamma^{(2)}(x) - \frac{23}{36}. \qquad (4.8)
\end{aligned}
$$

and

The MSSM experimental allowed region

Let us now elaborate a bit on the relevant region of the MSSM parameter space. We have determined from the analysis of eq.(4.4) and the generic constraints for the MSSM parameters stated in section 2.2.1 which is the relevant MSSM parameter region (Cf. Figs.4.5-4.9). It has been obtained in accordance with the CLEO data [132] on radiative $\bar{B}^0$ decays at $2\,\sigma$, imposing that non-SM contributions to the ρ-parameter be tempered by the relation

$$\delta\rho_{\rm new} \leq 0.003\,.$$

and having checked that the known necessary conditions for the non-existence of colour-breaking minima [84–87] are fulfilled. For definiteness, where M_H has to be fixed, we have chosen the value $M_{H^\pm} = 250\,GeV$ within the range:

$$m_t \lesssim M_{H^\pm} \lesssim 300\,GeV\,. \qquad (4.9)$$

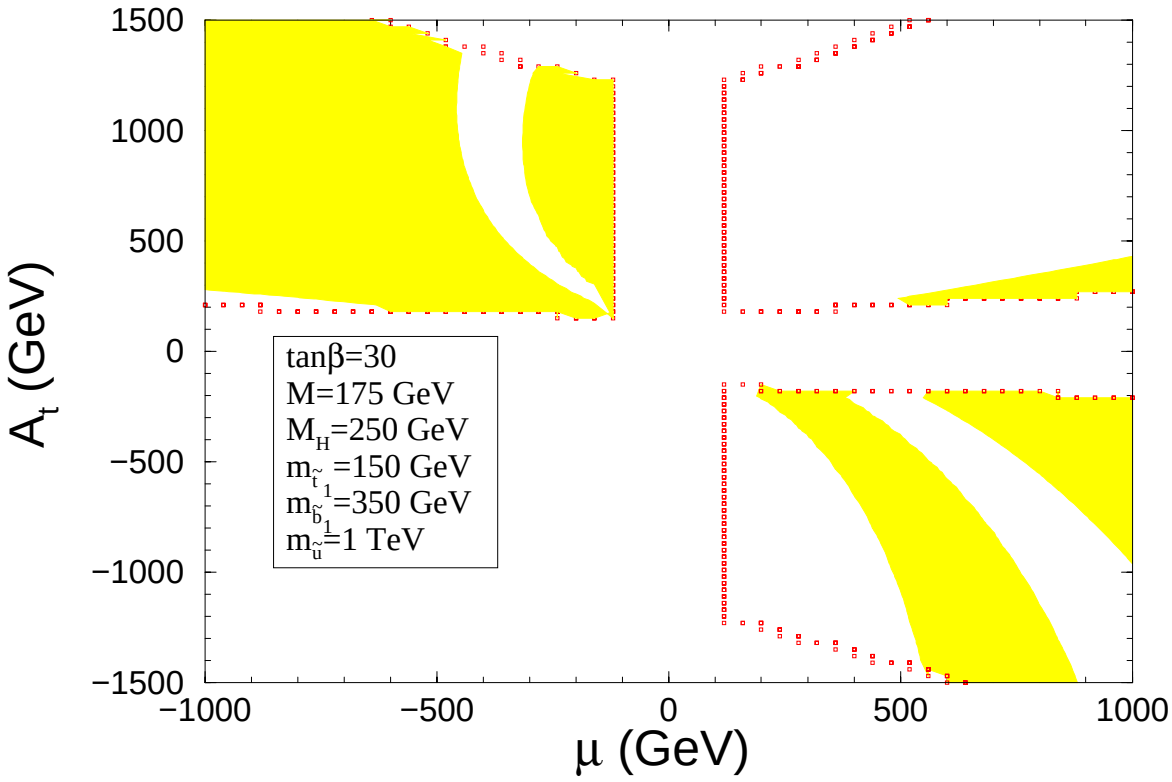

Figure 4.6: *Domains of the MSSM parameter space in the* (μ, A_t)*-plane allowed by* $b \to s\,\gamma$ *at* $2\,\sigma$ *level and the theoretical constraints explained in the text, for given values of the other parameters. The proper domains are the shaded ones.*

This window is especially significant in that the CLEO measurements [132] of $BR(b \to s\,\gamma)$ forbid most of this domain within the context of a generic 2HDM. However, within the MSSM the mass interval (4.9) is perfectly consistent with eq.(4.4) provided that relatively light stop and charginos ($\lesssim 200\,GeV$) occur [1]. Nevertheless, we shall also explicitly show the evolution of our results with M_H. As for the dependence on the QCD renormalization scale μ_{QCD}, following Ref. [132] we have entertained a variation of it in the segment $m_b/2 \leq \mu_{QCD} \leq 2\,m_b$ ($m_b = 5\,GeV$) and made allowance for an additional 10% theoretical uncertainty. On the whole this amounts to a $\gtrsim 30\%$ indeterminacy in the MSSM prediction. Even so, the constraint from $b \to s\,\gamma$ in combination with the others does project out a quite definite domain of the supersymmetric parameter space. For example, in Fig.4.5 we determine the allowed (shaded) region in the (μ, A_t)-plane for fixed values of the other parameters.

The information from Fig.4.5 is indeed relevant since, as it is apparent in the plot, the trilinear coupling A_t (a hot parameter modulating the SUSY-EW corrections) becomes strongly correlated with the higgsino mixing parameter μ, especially for low μ. The central vertical band around $\mu = 0$ is excluded by our (conservative) requirement that charginos should be heavier than $100\,GeV$. For $\mu < 0$, we find $A_t > 0$ in the permitted region by $\bar{B}^0$ decays; conversely, for $\mu > 0$, we find $A_t < 0$. Nevertheless, as showed in Fig. 4.6, this correlation may relax with a lower sbottom mass. The two sets of inputs defined in these two Figs. will be used later to illustrate the effects we will be studying.

Let us now explore a solution with $\mu < 0$ and give the allowed areas for the different MSSM parameters. We will use the set of inputs of Fig. 4.5. In Fig.4.7a we plot the proper area in the $(\tan\beta, A_t)$-plane and we see that there exists a sizable solution in the large $\tan\beta$ regime where to compute $\Gamma(H^+ \to t\,\bar{b})$. There is of course a low $\tan\beta$ solution, too, but in practice we shall only explore the large $\tan\beta$ option. This is because the MSSM corrections (4.67) other than the ordinary QCD corrections are not significant at low $\tan\beta$ (unless $\tan\beta < 1$, which is not so appealing from the theoretical point of view) and thus in that circumstance the potential SUSY nature of $H^\pm$ could not be disentangled from the measurement of its top

[1] Though the inclusion of the NLO effects on the charged Higgs corrected amplitude may considerably shift the range (4.9) up to higher values of M_H [131]

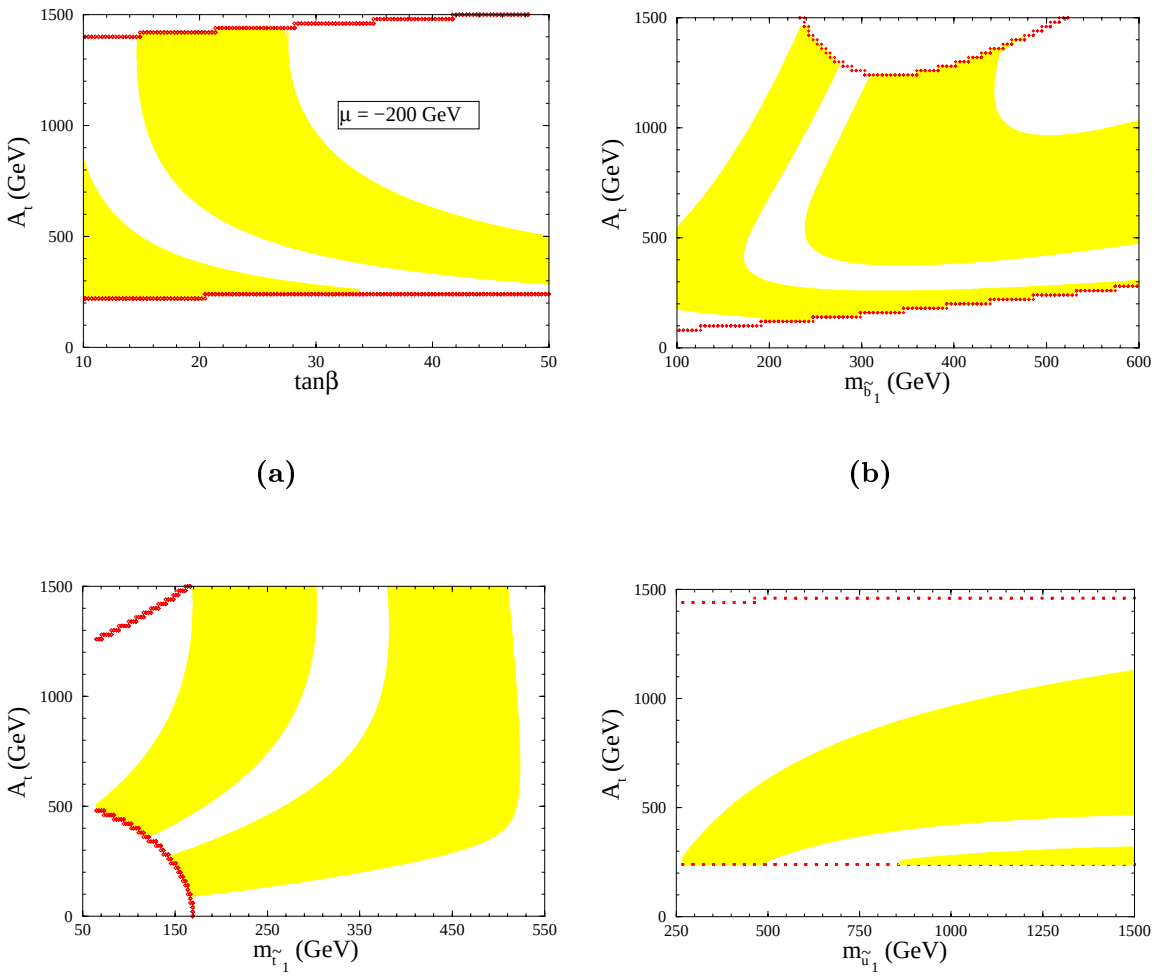

Figure 4.7: **(a)** *Domains of the MSSM parameter space in the* $(\tan\beta, A_t)$*-plane allowed by* $b \to s\gamma$ *at* 2σ *level and the theoretical constraints explained in the text, for given values of the other parameters. The proper domains are the shaded ones. Remaining inputs as in Fig.4.5.* **(b)** *As in (a), but for the* $(m_{\tilde{b}_1}, A_t)$*-plane.* **(c)** *As in (a), but for the* $(m_{\tilde{t}_1}, A_t)$*-plane.* **(d)** *As in (a), but for the* $(m_{\tilde{u}_1}, A_t)$*-plane.*

quark decay mode. In the large $\tan\beta$ subdomain relevant to our Higgs decay, namely

$$20 \lesssim \tan\beta \lesssim 50\,, \tag{4.10}$$

the bottom quark Yukawa coupling, λ_b, is comparable to the top quark Yukawa coupling, λ_t [2].

In Fig.4.7b-d we describe the correlation with the lightest squark masses. Specifically, in Figs.4.7b and 4.7c we project the $b \to s\,\gamma$ constraint onto the $(m_{\tilde{b}_1}, A_t)$ and $(m_{\tilde{t}_1}, A_t)$ planes, respectively. From the first one it is patent that there exists an essentially unlimited spectrum of heavy sbottom masses compatible with any stop trilinear coupling in the range $500\,GeV \lesssim A_t \lesssim 1\,TeV$ and without violating the $\delta\rho$ condition (6.23) – represented by the contour line hanging from above in Fig. 4.7a. This situation is different from that in Fig. 4.7c where there is a rather compact domain of proper $m_{\tilde{t}_1}$ values for each A_t. We emphasize that, contrary to the more commonly known result that holds at low $\tan\beta$, namely that the lightest stop allowed by radiative B-meson decays ought to be reachable at LEP 200, at high $\tan\beta$ the permissible values for $m_{\tilde{t}_1}$ are, instead, shifted away of the LEP 200 possibilities. As a matter of fact, the whole spectrum of sparticle masses that we use (including charginos) is unreachable by LEP 200. The variation of the A_t range with the squark masses of the first and second generation treated as degenerate, $m_{\tilde{u}}$, is shown to be mild in Fig. 4.7d.

We show that there is also a very mild variation of the allowed A_t range with M, m_{H^+}, m_b, m_t in Fig. 4.8.

Lastly, in Fig. 4.9 we show the allowed regions for $\mu > 0$ within the parameter set of Fig. 4.6. In that case there is a region with A_t also positive, as stated early. The large $\tan\beta$ region is more constrained (Fig. 4.9a), since $\tan\beta \lesssim 35$, in contrast to the squark masses regions that appear to be essentially unconstrained. In fact, $m_{\tilde{t}}$ should be larger than 150 GeV and for $A_t < 0$ $m_{\tilde{b}} \gtrsim 300$ GeV. The variations with the rest of parameters is uninteresting and we will no give it here.

[2] Theoretically, high values of $\tan\beta$ as in eq.(4.10) are well-motivated in the arena of widely different types of SUSY Yukawa coupling unification models [129, 133–136].

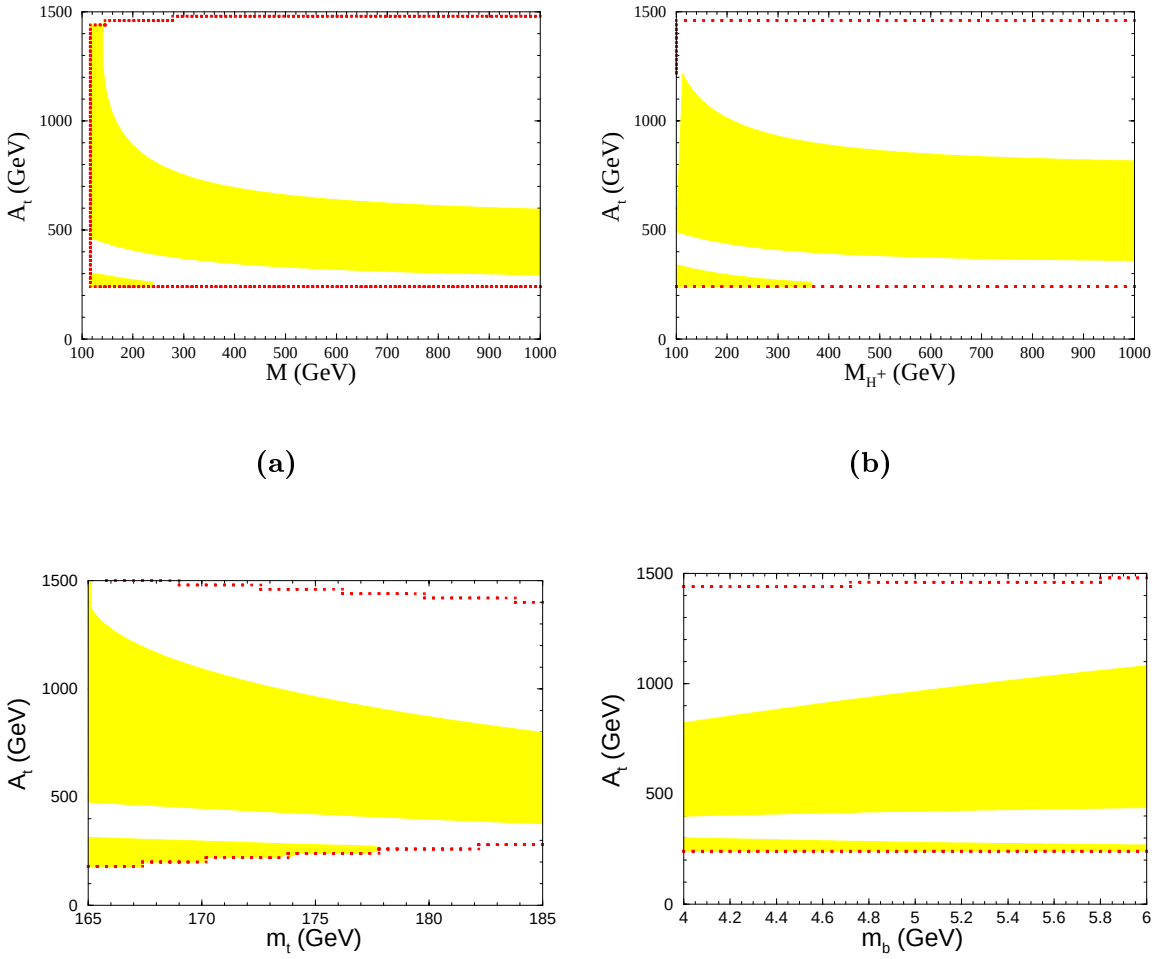

Figure 4.8: **(a)** *Domains of the MSSM parameter space in the* (M, A_t)*-plane allowed by* $b \to s\gamma$ *at* 2σ *level and the theoretical constraints explained in the text, for given values of the other parameters. The proper domains are the shaded ones. Remaining inputs as in Fig.4.5.* **(b)** *As in (a), but for the* (m_{H^+}, A_t)*-plane.* **(c)** *As in (a), but for the* (m_t, A_t)*-plane.* **(d)** *As in (a), but for the* (m_b, A_t)*-plane.*

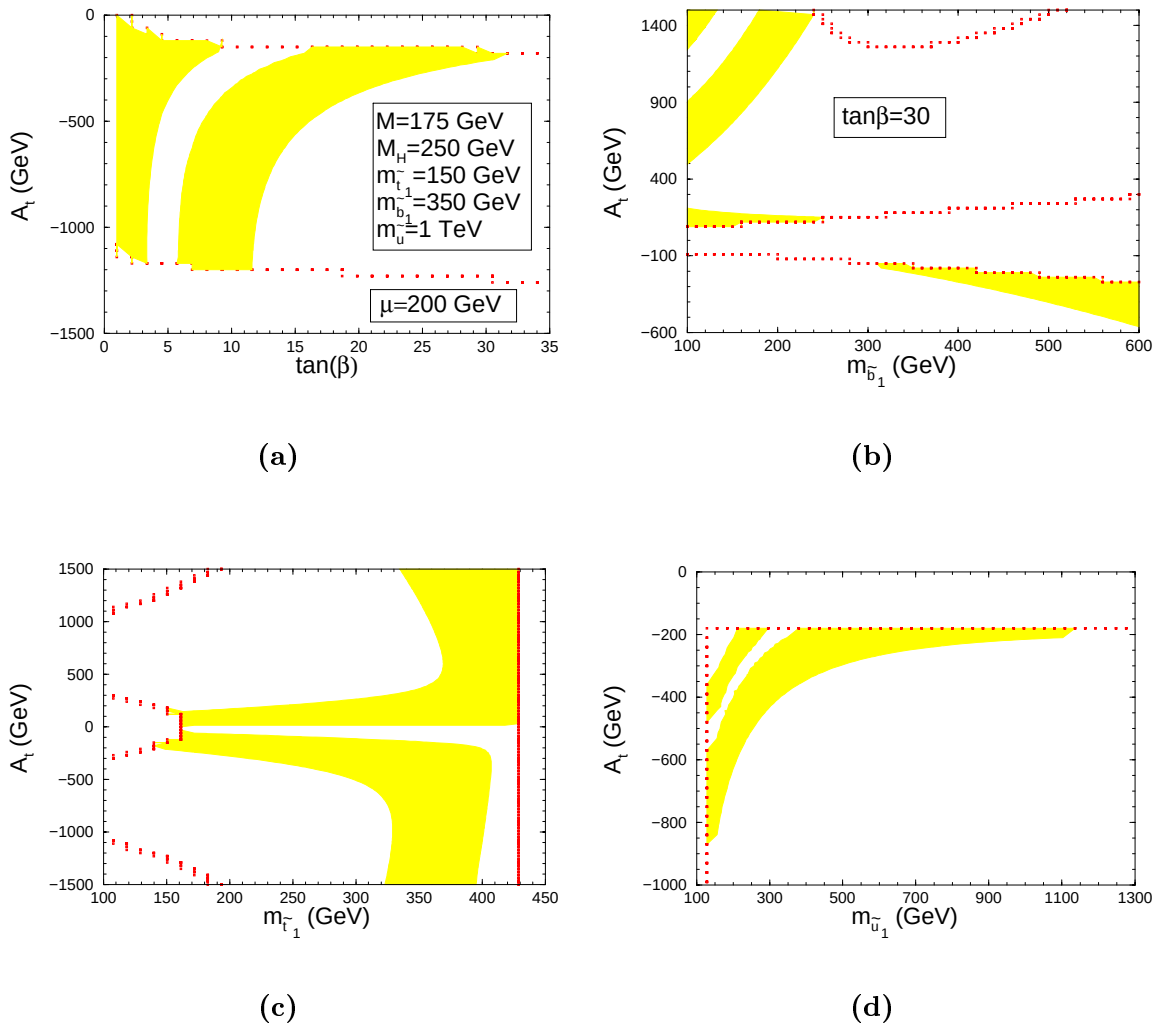

Figure 4.9: **(a)** *Domains of the MSSM parameter space in the* $(\tan\beta, A_t)$*-plane allowed by* $b \to s\,\gamma$ *at* $2\,\sigma$ *level and the theoretical constraints explained in the text, for given values of the other parameters. The proper domains are the shaded ones.* **(b)** *As in (a), but for the* $(m_{\tilde{b}_1}, A_t)$*-plane.* **(c)** *As in (a), but for the* $(m_{\tilde{t}_1}, A_t)$*-plane.* **(d)** *As in (a), but for the* $(m_{\tilde{u}_1}, A_t)$*-plane.*

4.3 Renormalization of $\Gamma(H^+ \to t\bar{b})$

Next, we shall address the calculation of the one-loop corrections to the partial width $H^+ \to t\bar{b}$ in the MSSM within the context of the on-shell renormalization framework [101, 105, 106], described in section 3.2.

Let us sketch the renormalization procedure affecting the parameters and fields related to the $t\,b\,H^{\pm}$-vertex, whose interaction Lagrangian was given on eq.(4.1). Following the procedure described in section 3.2 the renormalized MSSM Lagrangian $\mathcal{L} \to \mathcal{L}+\delta\mathcal{L}$ is obtained following a similar pattern as in the SM, i.e. by attaching multiplicative renormalization constants to each free parameter and field: $g_i \to (1+\delta g_i/g_i)g_i$, $\Phi_i \to Z_{\Phi_i}^{1/2}\Phi_i$.

4.3.1 The Mixing $H^{\pm} - W^{\pm}$. The δZ_{HW} counterterm

Doing this, one encounters that there exists a mixing term $H^{\pm} - W^{\pm}$ for the bare fields, which must be renormalized away for the physical fields $H^{\pm}$ and $W^{\pm}$ in the on-shell scheme. One can think of a counterterm δZ_{HW}, that obviously will be related to the doublet renormalization constants, $Z_{H_i} = 1 + \delta Z_{H_i}$, (see below) in such a way that the bare $W_{\mu}^{\pm}$ field can be written in terms of the counterterms and the physical fields:

$$W_{\mu}^{\pm} \to \left(Z_2^W\right)^{1/2} W_{\mu}^{\pm} \pm i\,\frac{\delta Z_{HW}}{M_W}\,\partial_{\mu} H^{\pm}\,. \tag{4.11}$$

Therefore, from the gauge piece of the bare lagrangian

$$\mathcal{L}_{Wbt} = \frac{g}{\sqrt{2}}\,W_{\mu}^{-}\,\bar{b}\,\gamma^{\mu}\,P_L\,t + \text{h.c.} \tag{4.12}$$

one obtains

$$\begin{aligned}\delta\mathcal{L}_{HW} &= -i\,\delta Z_{HW}\,\frac{g}{\sqrt{2}M_W}\,\partial_{\mu}H^{-}\,\bar{b}\,\gamma^{\mu}\,P_L\,t + \text{h.c.} \\ &\to \delta Z_{HW}\,\frac{g}{\sqrt{2}M_W}\,H^{-}\,\left[m_t\,\bar{b}\;P_R\,t - m_b\,\bar{b}\;P_L\,t\right] + \text{h.c.}\,,\end{aligned} \tag{4.13}$$

and in this way there is a contribution 'coming from this mixing' that adopts the form of the original vertex (4.1).

In the above expression (4.11), $Z_2^W = 1 + \delta Z_2^W$ is the usual $SU(2)_L$ gauge triplet renormalization constant. Furthermore, δZ_{HW} on eqs.(4.11)-(4.13) is a dimensionless constant

associated to the wave-function renormalization mixing among the bare $H^\pm$ and $W^\pm$ fields. Its relation with the doublet renormalization constants, $Z_{H_i} = 1 + \delta Z_{H_i}$, is the following:

$$\delta Z_{HW} = \sin\beta\cos\beta \left[\frac{1}{2}\left(\delta Z_{H_2} - \delta Z_{H_1}\right) + \frac{\delta\tan\beta}{\tan\beta}\right], \tag{4.14}$$

where $\delta\tan\beta$ is a counterterm associated to the renormalization of $\tan\beta$ (see below).

To fix this counterterm $-\delta Z_{HW}-$ in the on-shell scheme the no-mixing on-shell condition for the physical fields is imposed, that means that the renormalized mixed self energy $\hat{\Sigma}_{HW}(k^2)$ defined through:

$\hat{\Sigma}_{HW}(k^2) \equiv$ 

(4.15)

must vanish for $k^2 = M^2_{H^\pm}$:

$$\hat{\Sigma}_{HW}(k^2 = M^2_{H^\pm}) = 0 \tag{4.16}$$

Using the definition for the unrenormalized 2-point mixing Green function, $\Sigma_{HW}(k^2)$:

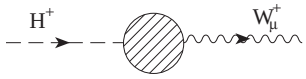

$\equiv -i\dfrac{k^\mu}{M_W}\Sigma_{HW}(k^2)$ (4.17)

and the unitary gauge one can easily find the expression for the counterterm δZ_{HW}.

From the gauge piece of the Lagrangian one easily finds the piece of the counterterm Lagrangian we are looking for:

$$\mathcal{L}_{UG} = -\frac{1}{4}F_{\mu\nu}F^{\mu\nu} + M_W^2 W_\mu^+ W^{-\mu} \rightarrow \mathcal{L}_{ct} = iM_W\delta Z_{HW}(W_\mu^-\partial^\mu H^+ - W_\mu^+\partial^\mu H^-)\,. \tag{4.18}$$

The corresponding renormalized 2-point Green function reads:

$$\frac{i}{k^2 - M^2_{H^\pm}}\left[k^\nu\frac{-i\Sigma_{HW}(k^2)}{M_W} + ik^\nu\ M_W^2\ \frac{\delta Z_{HW}}{M_W}\right]\frac{-i\left(g_{\mu\nu} - \frac{k_\mu k_\nu}{M_W^2}\right)}{k^2 - M_W^2}\,. \tag{4.19}$$

Thus, a renormalized self-energy can be defined as follows:

$$\hat{\Sigma}_{HW}(k^2) = \Sigma_{HW}(k^2) - M_W^2\delta Z_{HW} \tag{4.20}$$

where imposing the renormalization condition, eq 4.16, on $\hat{\Sigma}^{HW}(k^2)$ one finds:

$$\hat{\Sigma}_{HW}(M^2_{H^\pm}) = 0 \Longrightarrow \delta Z_{HW} = \frac{\Sigma_{HW}(M^2_{H^\pm})}{M_W^2}\,. \tag{4.21}$$

However, since we shall perform the rest of the calculation in the Feynman gauge [36,37, 72], it is worth considering the computation of δZ_{HW} in that gauge (see Sec. 4.3.1), where the discussion is slightly more complicated due to the presence of Goldstone bosons ($G^\pm$) leading to additional ($H^\pm - G^\pm$) mixing terms among the bare fields. The corresponding expression for δZ_{HW} is, however, formally identical in both gauges.

Peculiarities of the Feynman Gauge

As we carry out our calculation in the Feynman gauge, we would also like to perform the renormalization of the Higgs sector in that gauge. The Lagrangian is sketched as follows [36,37,72]:

$$L = L_C + L_{GF} + L_{FP} \,. \tag{4.22}$$

where L_{GF} stands for the gauge-fixing term in that gauge,

$$L_{GF} = -F^+ F^- + ... \qquad (F^\pm \equiv \partial^\mu W^+_\mu \mp i M_W G^+) \tag{4.23}$$

and $L_{FP} = \bar{\eta}^a \left(\partial F^a / \partial \theta^b\right) \eta^b$ is the Faddeev-Popov ghost Lagrangian constructed from FP and anti-FP Grassmann scalar fields $\eta, \bar{\eta}$. Since we are interested in the charged gauge-Higgs ($W^\pm - H^\pm$) and charged Goldstone-Higgs ($G^\pm - H^\pm$) mixing terms in that gauge, we have singled out just the relevant term on eq.(4.23).

The relationship with the original weak-eigenstate components on eq.2.10 is the following:

$$\begin{pmatrix} -H_1^+ \\ H_2^+ \end{pmatrix} = \begin{pmatrix} c_\beta & -s_\beta \\ s_\beta & c_\beta \end{pmatrix} \begin{pmatrix} G^+ \\ H^+ \end{pmatrix} . \tag{4.24}$$

As is well-known, although the classical Lagrangian, L_C, also contains a nonvanishing mixing among the weak gauge boson fields, $W^\pm$, and the Goldstone boson fields, $G^\pm$, namely

$$\mathcal{L}_{GW} = i M_W \, W^-_\mu \partial^\mu G^+ + \text{h.c.} \,, \tag{4.25}$$

the latter is cancelled (in the action) by a piece contained in L_{GF}. Now, after substituting the renormalization transformation for the Higgs doublets, eq.(3.4), on the Higgs boson kinetic term with $SU(2)_L \times U(1)_Y$ gauge covariant derivative, one easily projects out the following

relevant counterterms

$$\begin{aligned}\delta\mathcal{L} &= \delta Z_{H^\pm}\,\partial_\mu H^+\partial^\mu H^- + \delta Z_{G^\pm}\,\partial_\mu G^+\partial^\mu G^- \\ &+ \delta Z_{HG}\,\left(\partial_\mu H^-\partial^\mu G^+ + \text{h.c.}\right) + \delta Z_{HW}\,\left(iM_W\,W_\mu^-\partial^\mu H^+ + \text{h.c.}\right) + ...\end{aligned} \tag{4.26}$$

where

$$\begin{pmatrix}\delta Z_{H^\pm}\\ \delta Z_{G^\pm}\end{pmatrix} = \begin{pmatrix}c_\beta^2 & s_\beta^2\\ s_\beta^2 & c_\beta^2\end{pmatrix}\begin{pmatrix}\delta Z_{H_1}\\ \delta Z_{H_2}\end{pmatrix}\,, \tag{4.27}$$

and

$$\begin{aligned}\delta Z_{HG} &= s_\beta\,c_\beta\,\left(\delta Z_{H_2} - \delta Z_{H_1}\right)\,,\\ \delta Z_{HW} &= s_\beta\,c_\beta\,\left[\frac{1}{2}\left(\delta Z_{H_2} - \delta Z_{H_1}\right) + \frac{\delta\tan\beta}{\tan\beta}\right]\,.\end{aligned} \tag{4.28}$$

The renormalization transformation for the VEV's of the Higgs potential,

$$v_i \to Z_{H_i}^{1/2}(v_i + \delta v_i) = \left(1 + \frac{\delta v_i}{v_i} + \frac{1}{2}\,\delta Z_{H_i}\right)\,v_i\,, \tag{4.29}$$

implies that the counterterm to $\tan\beta$ is related to the fundamental counterterms in the Higgs potential by

$$\frac{\delta\tan\beta}{\tan\beta} = \frac{\delta v_2}{v_2} - \frac{\delta v_1}{v_1} + \frac{1}{2}\,\left(\delta Z_{H_2} - \delta Z_{H_1}\right)\,. \tag{4.30}$$

If one imposes the usual on-shell renormalization conditions for the A^0-boson, one has

$$\delta Z_{H_2} - \delta Z_{H_1} = -\frac{\tan\beta + \cot\beta}{M_Z^2}\,\Sigma_{AZ}(M_{A^0}^2)\,. \tag{4.31}$$

In addition, there is another mixing term between $H^\pm$ and $G^\pm$ originating from the mass matrix of the Higgs sector [137–140]. This one loop mixture is contained in:

$$V^b = \left(\begin{array}{cc}H^{+b} & G^{+b}\end{array}\right)\begin{pmatrix}M_{H^\pm}^{b\,2} & \frac{t_0^b}{\sqrt{2}v^b}\\ \frac{t_0^b}{\sqrt{2}v^b} & \frac{t_1^b}{\sqrt{2}v^b}\end{pmatrix}\begin{pmatrix}H^{-b}\\ G^{-b}\end{pmatrix}\,, \tag{4.32}$$

where we have attached a superscript b to bare quantities, and t_i are the tadpole counterterms

$$\begin{aligned}t_0 &= -\sin\left(\beta-\alpha\right)\;t_{H^0} + \cos\left(\beta-\alpha\right)\;t_{h^0}\\ t_1 &= \sin\left(\beta-\alpha\right)\;t_{h^0} + \cos\left(\beta-\alpha\right)\;t_{H^0}\,.\end{aligned} \tag{4.33}$$

We are now ready to find an expression for the mixed 2-point Green functions (Figs.4.10a and 4.10b). As the mixing Lagrangian between $H^\pm$ and $W^\pm$ on eq. (4.18) is the same as on

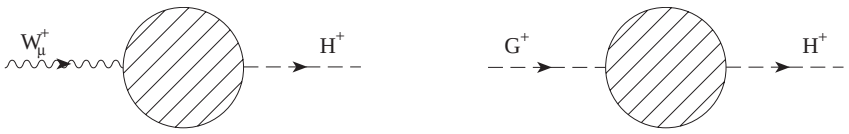

Figure 4.10: *The mixed blobs W^+-H^+ and G^+-H^+ at any order of perturbation theory.*

eq. (4.26), the 2-point Green function will have the same expression (4.19) but with the $W^\pm$ propagator in the Feynman gauge, namely:

$$\frac{i}{k^2 - M_{H^\pm}^2}\left[k^\nu \frac{-i\Sigma_{HW}(k^2)}{M_W} + ik^\nu\, M_W^2\, \frac{\delta Z_{HW}}{M_W}\right]\frac{-ig_{\mu\nu}}{k^2 - M_W^2}$$
$$= \frac{i}{k^2 - M_{H^\pm}^2}\left[k_\mu \frac{-i\hat{\Sigma}_{HW}(k^2)}{M_W}\right]\frac{-i}{k^2 - M_W^2} \equiv \Delta_\mu^{HW}\,. \tag{4.34}$$

Next we impose $\hat{\Sigma}_{HW}(M_{H^\pm}^2) = 0$ as before, leading to the same formal expression for δZ_{HW} as in eq.(4.21). However, as a new ingredient, we now have the mixed $H^\pm - G^\pm$ self-energy:

$$\frac{i}{k^2 - M_{H^\pm}^2}\left(-i\Sigma_{HG}(k^2) + ik^2\delta Z_{HG} - i\frac{t_0^b}{\sqrt{2}v^b}\right)\frac{i}{k^2 - M_W^2}\,. \tag{4.35}$$

This allows us to define renormalized self-energies, (4.20) and

$$\hat{\Sigma}_{HG}(k^2) = \Sigma_{HG}(k^2) - k^2\delta Z_{HG} + \frac{t_0^b}{\sqrt{2}v^b}\,. \tag{4.36}$$

The mixed self-energies $\hat{\Sigma}_{HW}(k^2)$ and $\hat{\Sigma}_{HG}(k^2)$ obey the following Slavnov-Taylor identity:

$$k^2\hat{\Sigma}_{HW}(k^2) - M_W^2\hat{\Sigma}_{HG}(k^2) = 0\,. \tag{4.37}$$

This identity is derived from a BRS transformation involving the Green function constructed with an anti-FP field and the charged Higgs field: $< 0|\delta_{BRS}\,(\bar{\eta}^+\, H^+)|0 >= 0$. Following the standard procedure [141] one immediately gets:

$$< 0|F^+\, H^+|0 >=< 0|\partial^\mu W_\mu^- + H^+ - iM_W\, G^+ H^+|0 >= 0\,, \tag{4.38}$$

which in momentum space reads

$$k^\mu\, \Delta_\mu^{HW} + M_W\, \Delta^{HG} = 0 \tag{4.39}$$

with

$$\Delta^{HG} \equiv \frac{i}{k^2 - M^2_{H^\pm}} \left[-i\,\hat{\Sigma}_{HG}(k^2)\right] \frac{i}{k^2 - M^2_W}\,. \tag{4.40}$$

Clearly, eq.(4.39) implies eq.(4.37). The latter identity guarantees that the contribution to our decay $t \to H^+ b$ from the two diagrams in Figs.4.10a and 4.10b vanishes since no mixing is generated among the physical boson $H^\pm$ and the renormalized fields $G^\pm$ and $W^\pm$: $\hat{\Sigma}_{HG}(M^2_{H^\pm}) = \hat{\Sigma}_{HW}(M^2_{H^\pm}) = 0$. There is of course another Slavnov-Taylor identity, derived in a similar manner, which insures that the renormalized mixing between $G^\pm$ and $W^\pm$ also vanishes. Thus we have proven that the expression for δZ_{HW} is formally the same in both unitary and Feynman gauges, but that in the latter gauge one must take into account the additional renormalization of the mixed self-energy Σ_{HG}.

4.3.2 The $\tan\beta$ counterterm

Let us consider next the renormalization of the Higgs potential in the MSSM, eq.(2.15) [77–81]. After expanding the neutral components H^0_1 and H^0_2 around their VEV's v_1 and v_2, the one-point functions of the resulting CP-even fields are required to vanish, i.e. the tadpole counterterms are constrained to exactly cancel the tadpole diagrams, so that the renormalized tadpoles are zero and the quantities $v_{1,2}$ remain as the VEV's of the renormalized Higgs potential. Notwithstanding, at this stage a prescription to renormalize $\tan\beta = v_2/v_1$,

$$\tan\beta \to \tan\beta + \delta\tan\beta\,, \tag{4.41}$$

is still called for. There are many possible strategies. The ambiguity is related to the fact that this parameter is just a Lagrangian parameter and as such it is not a physical observable. Its value beyond the tree-level is renormalization scheme dependent. (The situation is similar to the definition of the weak mixing angle θ_W, or equivalently of $\sin^2\theta_W$.) However, even within a given scheme, e.g. the on-shell renormalization scheme, there are some ambiguities that must be fixed. For example, we may wish to define $\tan\beta$ in a process-independent ("universal") way as the ratio v_2/v_1 between the true VEV's after renormalization of the Higgs potential [77–81, 137–140]. In this case a consistent choice (i.e. a choice capable of

renormalizing away the tadpole contributions) is to simultaneously shift the VEV's and the mass parameters of the Higgs potential, eq.(2.15),

$$\begin{aligned} v_i &\to Z_{H_i}^{1/2}(v_i + \delta v_i)\,, \\ m_i^2 &\to Z_{H_i}^{\frac{1}{2}}\,(m_i^2 + \delta m_i^2)\,, \\ m_{12}^2 &\to Z_{H_1}^{\frac{1}{2}}\,Z_{H_2}^{\frac{1}{2}}\,(m_{12}^2 + \delta m_{12}^2)\,, \end{aligned} \tag{4.42}$$

$(i = 1, 2)$ in such a way that $\delta v_1/v_1 = \delta v_2/v_2$. This choice generates the following counterterm for $\tan\beta$ in that scheme (Cf. Sec. 4.3.1):

$$\frac{\delta \tan\beta}{\tan\beta} = \frac{1}{2}\,(\delta Z_{H_2} - \delta Z_{H_1})\,. \tag{4.43}$$

Nevertheless, this procedure looks very formal and one may eventually like to fix the on-shell renormalization condition on $\tan\beta$ in a more physical way, i.e. by relating it to some concrete physical observable, so that it is the measured value of this observable that is taken as an input rather than the VEV's of the Higgs potential. Following this practical attitude, we choose as a physical observable the decay width of the charged Higgs boson into τ-lepton and associated neutrino: $H^+ \to \tau^+\nu_\tau$. This should be a good choice, because:

- When $H^+ \to t\bar{b}$ is allowed, the decay $H^+ \to \tau^+\nu_\tau$ is never below 5% for large $\tan\beta$ though $H^+ \to t\bar{b}$ is the dominant decay mode;

- From the experimental point of view there is a well-defined method to separate the final state τ's originating from H^+-decay from those coming out of the conventional decay $W^+ \to \tau^+\nu_\tau$, so that $H^+ \to \tau^+\nu_\tau$ should be physically accessible.

- The interaction Lagrangian describing the decay $H^+ \to \tau^+\nu_\tau$ is directly proportional to $\tan\beta$,

$$\mathcal{L}_{H\tau\nu} = \frac{g\, m_\tau \tan\beta}{\sqrt{2} M_W}\, H^-\, \bar{\tau}\, P_L\, \nu_\tau + \text{h.c.}\,, \tag{4.44}$$

  and the relevant decay width is proportional to $\tan^2\beta$. Whether in the α-scheme or in the G_F-scheme, it reads:

$$\Gamma(H^+ \to \tau^+\nu_\tau) = \frac{\alpha m_{\tau^+}^2 M_{H^+}}{8 M_W^2 s_W^2}\tan^2\beta = \frac{G_F m_{\tau^+}^2 M_{H^+}}{4\pi\sqrt{2}}\tan^2\beta(1 - \Delta r^{MSSM}), \tag{4.45}$$

where we have used the relation (3.29). By measuring this decay width one obtains a physical definition of $\tan\beta$ which can be used beyond the tree-level. A combined measurement of $M_{H^\pm}$ and $\tan\beta$ from charged Higgs decaying into τ-lepton in a hadron collider has been described in the literature [142–145] by comparing the size of the various signals for charged Higgs boson production, such as the multijet channels accompanied by a τ-jet or a large missing p_T, and the two-τ-jet channel. For the upgraded Tevatron, the conventional mechanisms $gg(q\bar{q}) \to t\bar{t}$ followed by an offshell top 'decay' $t \to H^+ b$ are being studied [44, 45], and as argued before this associated production mechanism can be comparable or larger than the usual single top production mechanism $q\bar{q} \to W^* \to t\bar{b}$.

Insofar as the determination of the counterterm $\delta\tan\beta$ in our scheme, it can be fixed unambiguously from our Lagrangian definition of $\tan\beta$ on eq.(4.44) and the renormalization procedure described above. It is straightforward to find:

$$\frac{\delta\tan\beta}{\tan\beta} = \frac{\delta v}{v} - \frac{1}{2}\delta Z_{H^\pm} + \cot\beta\,\delta Z_{HW} + \Delta_\tau\,. \tag{4.46}$$

Notice the appearance of the vacuum counterterm

$$\frac{\delta v}{v} = \frac{1}{2}\frac{\delta v^2}{v^2} = \frac{1}{2}\frac{\delta M_W^2}{M_W^2} - \frac{1}{2}\frac{\delta g^2}{g^2}\,, \tag{4.47}$$

which is associated to $v^2 = v_1^2 + v_2^2$. The last term on eq.(4.46),

$$\Delta_\tau = -\frac{\delta m_\tau}{m_\tau} - \frac{1}{2}\delta Z_L^{\nu_\tau} - \frac{1}{2}\delta Z_R^{\tau} - F_\tau\,, \tag{4.48}$$

is the (finite) process-dependent part of the counterterm. Here $\delta m_\tau/m_\tau$, $\delta Z_L^{\nu_\tau}$ and δZ_R^{τ} are obtained from eqs.(3.27) and (3.27) (with $m_{\nu_\tau} = 0$); they represent the contribution from the mass and wave-function renormalization of the (ν_τ, τ)-doublet, including the finite renormalization of the neutrino leg. Finally, F_τ on eq.(4.48) is the form factor describing the vertex corrections to the amplitude of $H^+ \to \tau^+\nu_\tau$.

On comparing eqs.(4.43) and (4.46) we see that the first definition of $\tan\beta$ appears as though it is free from process-dependent contributions. In practice, however, process-dependent terms are inevitable, irrespective of the definition of $\tan\beta$. In fact, the definition of $\tan\beta$ where $\delta v_1/v_1 = \delta v_2/v_2$ [146] will also develop process-dependent contributions, as

can be seen by trying to relate the "universal" value of $\tan\beta$ in that scheme with a physical quantity directly read off some physical observable. For instance, if M_{A^0} is heavy enough, one may define $\tan\beta$ as follows:

$$\frac{\Gamma(A^0 \to b\,\bar{b})}{\Gamma(A^0 \to t\,\bar{t})} = \tan^4\beta\,\frac{m_b^2}{m_t^2}\left(1-\frac{4\,m_t^2}{M_{A^0}^2}\right)^{-1/2}\left[1+4\left(\frac{\delta v_2}{v_2}-\frac{\delta v_1}{v_1}\right)\right.$$
$$\left.+2\left(\frac{\delta m_b}{m_b}+\frac{1}{2}\delta Z_L^b+\frac{1}{2}\delta Z_R^b-\frac{\delta m_t}{m_t}-\frac{1}{2}\delta Z_L^t-\frac{1}{2}\delta Z_R^t\right)+\delta V\right]\,, \quad (4.49)$$

where we have neglected $m_b^2 \ll M_{A^0}^2$, and δV stands for the vertex corrections to the decay processes $A^0 \to b\,\bar{b}$ and $A^0 \to t\,\bar{t}$. Since the sum of the mass and wave-function renormalization terms along with the vertex corrections is UV-finite, one can consistently choose $\delta v_1/v_1 = \delta v_2/v_2$ leading to eq.(4.43). Hence, deriving $\tan\beta$ from eq.(4.49) unavoidably incorporates also some process-dependent contributions.

Any definition of $\tan\beta$ is in principle as good as any other; and in spite of the fact that the corrections themselves may show some dependence on the choice of the particular definition [147], the physical observables should not depend at all on that choice. However, it can be a practical matter what definition to use in a given situation. For example, our definition of $\tan\beta$ given on eq.(4.45) may be more adequate for $M_{H^\pm} < m_t - m_b$ and large $\tan\beta$, since then $H^+ \to \tau^+\,\nu_\tau$ is the dominant decay of H^+, but, as will be seen later, it is also useful when $M_{H^\pm} > m_t - m_b$ and $\tan\beta$ is large. Notwithstanding, the definition based on eq.(4.49) requires a large value of $\tan\beta$ (to avoid an impractical suppression of the $b\,\bar{b}$ mode) and, in order to be operative, it requires, as well, a much heavier charged Higgs boson, since $M_{H^\pm} \simeq M_{A^0} > 2\,m_t$ when the decay $A \to t\bar{t}$ is kinematically open in the MSSM. (Use of light quark final states would, of course, be extremely difficult from the practical point of view.)

4.3.3 The renormalized $t\,b\,H^\pm$-vertex

Within our context, we use eq.(4.46) for $\delta\tan\beta/\tan\beta$ in order to compute the one-loop corrections to our decay $t \to H^+\,b$. Putting all the pieces together, the counterterm Lagrangian for the vertex $t\,b\,H^+$ follows right away from the bare Lagrangian (4.1) after re-expressing

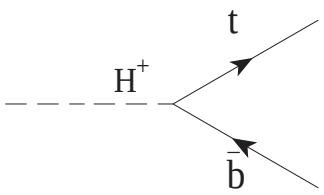

Figure 4.11: *The lowest-order Feynman diagram for the charged Higgs decay* $H^+ \to t\bar{b}$.

everything in terms of renormalized parameters and fields in the on-shell scheme. It takes on the form :

$$\delta\mathcal{L}_{Hbt} = \frac{g}{\sqrt{2}\,M_W}\, H^+\,\bar{t}\,[\delta G_L\; m_t\,\cot\beta\; P_L + \delta G_R\; m_b\,\tan\beta\, P_R]\; b + \text{h.c.}\,, \tag{4.50}$$

with

$$\begin{aligned}
\delta G_L &= \frac{\delta m_t}{m_t} - \frac{\delta v}{v} + \frac{1}{2}\,\delta Z_{H^+} + \frac{1}{2}\,\delta Z_L^b + \frac{1}{2}\,\delta Z_R^t - \frac{\delta\tan\beta}{\tan\beta} + \delta Z_{HW}\;\tan\beta\,,\\
\delta G_R &= \frac{\delta m_b}{m_b} - \frac{\delta v}{v} + \frac{1}{2}\,\delta Z_{H^+} + \frac{1}{2}\,\delta Z_L^t + \frac{1}{2}\,\delta Z_R^b + \frac{\delta\tan\beta}{\tan\beta} - \delta Z_{HW}\;\cot\beta\,,
\end{aligned} \tag{4.51}$$

and where we have set $V_{tb} = 1$.

4.4 One-loop Corrected $\Gamma(H^+ \to t\bar{b})$ in the MSSM

In the following we will describe the relevant electroweak one-loop supersymmetric diagrams entering the amplitude of $H^+ \to t\bar{b}$ in the MSSM. At tree-level, the only Feynman diagram is the one in Fig. 4.11. At one-loop, we have the diagrams exhibited in Figs. 4.12-4.17. The computation of the one-loop diagrams requires to use the full structure of the MSSM Lagrangian. The explicit form of the most relevant pieces of this Lagrangian, together with the necessary SUSY notation, is provided in Sec. 2.2.1.

Specifically, Fig. 4.12 shows the SUSY vertices involving gluinos, squarks, charginos and neutralinos. In all these diagrams a sum over all indices is taken for granted. The supersymmetric Higgs particles of the MSSM and Goldstone bosons (in the Feynman gauge) contribute a host of one-loop vertices as well (see Fig. 4.13). As for the various self-energies, they will be treated as counterterms to the vertices. Their contribution is dictated by the Lagrangian

(4.50). Thus, Fig. 4.14 displays the counterterms $C_{b0} - C_{t4}$ generated from the external bottom and top quark lines; they include contributions from supersymmetric particles, Higgs bosons and Goldstone bosons. Similarly, Fig. 4.16 contains the counterterms $C_{H1} - C_{H6}$ associated to the self-energy of the external charged Higgs boson. A variant of the latter contribution is the mixed $W^+ - H^+$ self-energy counterterms $C_{M1} - C_{M4}$ shown in Fig. 4.17.

Although we have displayed only the process dependent diagrams, the full analysis should also include the SUSY and Higgs/Goldstone boson contributions to the various universal vacuum polarisation effects comprised in our counterterms. However, the calculation of all these pieces has already been discussed in detail long ago in the literature [73–76, 148] and thus the lengthy formulæ accounting for these results will not be explicitly quoted here. Their contribution is not $\tan\beta$-enhanced, but since we wish to compute the full supersymmetric contribution in the relevant regions of the MSSM parameter space, those effects will be included in our numerical code.

Next let us report on the contributions from the various vertex diagrams and counterterms in the on-shell renormalization scheme. The generic structure of any renormalized vertex function, Λ, in Figs.4.12-4.13 can be expressed in terms of two form factors H_R, H_L. Therefore, on making use of the formulae of Section 4.3, one immediately finds:

$$\Lambda = \frac{i\,g}{\sqrt{2}\,M_W}\left[m_t\,\cot\beta\,(1+G_L)\,P_L + m_b\,\tan\beta\,(1+\Lambda_R)\,P_R\right]\,, \tag{4.52}$$

where

$$\begin{aligned} G_L &= H_R + \frac{\delta m_t}{m_t} + \frac{1}{2}\,\delta Z_L^b + \frac{1}{2}\,\delta Z_R^t - \Delta_\tau \\ &- \frac{\delta v^2}{v^2} + \delta Z_{H^+} + (\tan\beta - \cot\beta)\,\delta Z_{HW}\,, \\ G_R &= H_L + \frac{\delta m_b}{m_b} + \frac{1}{2}\,\delta Z_L^t + \frac{1}{2}\,\delta Z_R^b + \Delta_\tau\,. \end{aligned} \tag{4.53}$$

In the following the analytical contributions to the vertex form factors and counterterms will be specified diagram by diagram.